Electronic Structure Evolution during Martensitic Phase Transition in All-*d*-Metal Heusler Compounds: The Case of Pd_2MnTi

Guijiang Li(李贵江)[1*], Gang Wang(王刚)[2], and Enke Liu(刘恩克)[2*]

[1]*College of Materials Science and Engineering, Nanjing Tech University, Nanjing 211816, China*
[2]*Beijing National Laboratory for Condensed Matter Physics, Institute of Physics, Chinese Academy of Sciences, Beijing 100190, China*

(Received 30 August 2024; accepted manuscript online 22 October 2024)

Taking Pd_2MnTi as a representative example, we systematically investigate and theoretically reveal the electronic structure evolution during martensitic phase transition in all-*d*-metal Heusler compounds. The calculation and theoretical analysis suggest that Pd_2MnTi is not stable in cubic structure and prone to transform to low-symmetric tetragonal structure. By tetragonal deformation, the shrinkage of lattice parameters and the decrease of symmetry promote the electron accumulation between Pd and its first nearest neighboring Ti atom, resulting in the increasing covalent hybridization. The occurrence of pseudogap in density of states of tetragonal Pd_2MnTi near the Fermi level also verifies the enhancement of covalent bond. Comparatively, the stronger interatomic bond in tetragonal Pd_2MnTi, i.e., covalent bond here, would strengthen interatomic coupling and consequently lower the energy of the material. By the martensitic phase transition, more stable states in energy are achieved. Thus, based on the analysis of electronic structure evolution, the nature of martensitic phase transition is a process wherein symmetry breaking weakens the original weak chemical bonds in high-symmetric parent phase and induces the strong chemical bond to lower the energy of the materials and to achieve a more stable state. This study could help to deepen the understanding of martensitic phase transition and the exploration of novel materials for potential technical applications.

DOI: 10.1088/0256-307X/41/11/117102

All-*d*-metal Heusler compounds are a particularly appealing family of functional materials,[1] which were firstly designed and prepared by Wei *et al.* in 2015.[2] The general formula of all-*d*-metal Heusler compounds is X_2YZ, where usually X and Y are late transition metals, and Z is early transition metal.[2–7] In well-known conventional X_2YZ-type Heusler compounds, Z is main-group element. Thus, all-*d*-metal Heusler compounds can be considered as products of replacing the main-group element in conventional Heusler compounds by early transition metals. Owing to the similarity between main-group elements and early transition metals, all-*d*-metal Heusler compounds inherit both structural characteristic and functional properties of conventional X_2YZ-type Heusler compounds.[1] Comparative analyses of their chemical bonds indicate that the *d*–*d* interatomic hybridization is dominated in all-*d*-metal Heusler compounds since all consistent atoms are transition metals.[3,4,8–10] All-*d*-metal Heusler compounds are endowed with many exceptional features by virtue of this transition from *p*–*d* covalent-type coupling in conventional Heusler compounds to *d*–*d* metallic hybridization. For example, owing to the improved metallic bond, the experimental and theoretical investigations suggested that the ductility in this kind of materials is greatly improved.[10–14] This enhancement enables all-*d*-metal Heusler compounds high fatigue life and good application future. In all-*d*-metal Heusler compounds, large lattice volume shrinkage was experimentally observed when the materials undergo the phase transformation.[15] This large volume change works as an essential requirement of colossal elastocaloric effect in ferroelastic Ni–Mn–Ti–B compounds[14] and the important influence factor on low-pressure-induced giant barocaloric effect in Ni–Co–Mn–Ti compounds.[16] In materials having martensitic phase transition, the broken symmetry of crystal structures changes the spin-polarization level and gives rise to different magnetic moments in solids. Moreover, some of the all-*d*-metal Heusler compounds are ferromagnetic in cubic structures. Owing to the phase transformation, the magnetic moment would also change. The metamagnetic martensitic phase transition would give rise to magnetocaloric effect.[17,18] Experimentally, giant magnetocaloric response was observed in Ni–Co–Mn–Ti all-*d*-metal Heusler compounds.[2,12,19,20] Importantly, the indicators for describing the performance of the abovementioned elastocaloric effect, barocaloric effect, and magnetocaloric effect in all-*d*-metal Heusler compounds are superior to those in traditional Heusler materials. The improved ductility and outstanding multicaloric effects make all-*d*-metal Heusler compounds popular in condensed matter physics. Although great achievements have been made in experimental investigations, the theoretical research on the electronic structure evolution and correspondingly the nature of martensitic phase transition is little. Thus, it

*Corresponding authors. Email: guijiangli@njtech.edu.cn; ekliu@iphy.ac.cn
© 2024 Chinese Physical Society and IOP Publishing Ltd

is desired to investigate the electronic structure evolution during martensitic phase transformation in theory.

In this study, the Pd_2MnTi is selected as a representative sample to investigate the electronic structure evolution during martensitic phase transition. The existing cubic phase and tetragonal phases with different lattice distortions in Pd_2MnTi provides an ideal platform to reveal the electronic structure evolution and the nature of martensitic phase transition. Hopefully, such a study would help to deepen the understanding of the nature of martensitic phase transition, to explore novel martensitic phase transition materials and to optimize their properties for functional applications.

The investigations in literature[21] suggested that the ground state of parent cubic Pd_2MnTi is ferromagnetic and stable in the $L2_1$-type structure (space group $Fm\bar{3}m$, No. 225). In the $L2_1$-type cubic structure, the two equivalent Pd atoms lie on the 8*c* Wyckoff sites, (0.25, 0.25, 0.25) and (0.75, 0.75, 0.75). For the Wyckoff sites 4*b* (0.5, 0.5, 0.5) and 4*a* (0, 0, 0), they are occupied by Mn and Ti, respectively. When martensitic phase transition occurs, Pd_2MnTi will transform from cubic structure to tetragonal structure, i.e., $L1_0$-type tetragonal structure (space group $P4/mmm$, No. 123). In the $L1_0$-type tetragonal structure, the atoms Pd, Mn, and Ti are located at Wyckoff sites 4*d* (0, 0.5, 0.25), 2*b* (0, 0, 0.5), and 2*a* (0, 0, 0), in that order. Based on the above-mentioned cubic and tetragonal structures, the theoretical calculations were carried out by CASTEP code to reveal the electronic structure evolution and the nature of martensitic phase transition. The same method as those in published work was adopted to calculate elastic constants and related moduli.[3,4] Electron localization function distributions were calculated to vividly reveal the characteristics of chemical bonds in Pd_2MnTi.[22,23] Therein, 1×10^{-6} eV/atom was chosen as the energy convergence threshold. The cutoff density plane wave was 500 eV. The ultrasoft pseudopotential was used to characterize the interactions between the atomic core and the valence electrons.[24] The Perdew–Burke–Ernzerhof (PBE) functional in generalized gradient approximation (GGA) was used for all calculations in this study to determine the electrons' exchange-correlation energy.[25] In the cubic structure, the *k*-point mesh of $15 \times 15 \times 15$ was chosen. The *k*-point meshes in the tetragonal structure depend on the lattice distortion level, i.e., c/a values.

To discuss possibility of the martensitic phase transition in Pd_2MnTi, the dependence of energy on lattice volumes and lattice distortion levels was considered and theoretically calculated. Details can be seen in Fig. 1. First, in Fig. 1(a), two local minima are discernible around lower lattice distortion zone ($c/a \approx 0.85$) and higher c/a zone ($c/a \approx 1.4$). Comparatively, the minimum at higher c/a zone shows lower energy, meaning a more stable state. The energy difference between cubic phase and tetragonal phase with large c/a is about 0.24 eV. Herein, both the lattice distortion level and energy difference between the two phases in Pd_2MnTi are comparable with the reported data in known martensitic phase transition materials.[26] Thus, possible martensitic phase could be expected in Pd_2MnTi. Additionally, the energy difference between cubic phase and the tetragonal phase with $c/a \approx 0.85$ is about 0.05 eV. Thus, the tetragonal phase possessing smaller lattice distortion is metastable. For Pd_2MnTi, the coexistence of cubic phase, metastable and stable tetragonal phases provides an ideal platform to investigate the electronic structure evolution during martensitic phase transition.

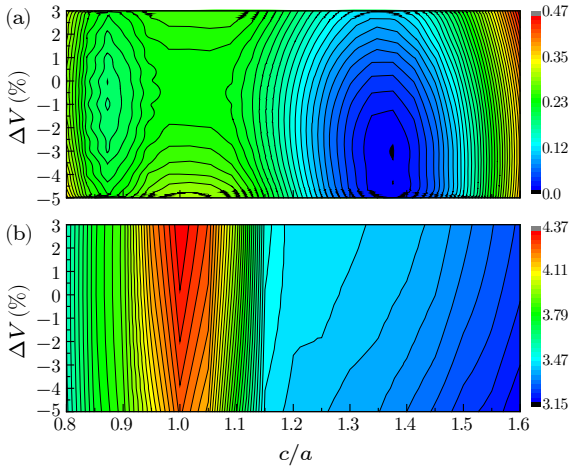

Fig. 1. (a) Total energy contour map (eV/f.u.) of Pd_2MnTi with respect to lattice distortion level (c/a) and change in volume. Zero energy corresponds to $c/a = 1.4$ and a volume change of −3%. (b) Pd_2MnTi's total moment contour map (μ_B/f.u.) with respect to lattice distortion level and change in volume.

Importantly, during the transformation from cubic phase under ground state to stable tetragonal phase, the lattice volume change ratio is about −3% [see Fig. 1(a) for details]. This value can be compared with available experimental and theoretical results about other all-*d*-metal Heusler compounds.[8,14,15,27] Experimentally, this kind of large volume change was considered as the crucial factor of colossal elastic-caloric effect[14] and large barocaloric effect.[16] Meanwhile, in Fig. 2(b), one can find that the magnetic moment would become smaller when the c/a is not 1, whether the c/a becomes smaller or higher. The changes of magnetic moment indicate that the martensitic phase transition is metamagnetic, which could result in magnetocaloric effect in Pd_2MnTi. Experiments in Fe-Kagome single crystals also suggest that the metamagnetic transition could help magnetic materials to reach the more stable state in energy.[28,29] Based on the martensitic phase transition character, the possible multicaloric effects in Pd_2MnTi would make it attractive candidate material for solid-state refrigeration application like the cases in MM'X-type materials.[30,31] Further experiments are encouraged to verify current theoretical prediction on the possibility of martensitic phase transition.

To further confirm the relative stability of cubic phase and tetragonal phase with higher c/a, the phonon dispersions and correspondingly site projected phonon density of states were calculated. They could also help to reveal the

physical mechanism. Herein, the phonon dispersions of cubic ($c/a = 1$) and stable tetragonal Pd_2MnTi ($c/a = 1.4$) are shown in Figs. 2(a) and 2(c), respectively. Generally, there are no observed imaginary frequencies throughout the whole Brillouin zone in Figs. 2(a) and 2(c), indicating the dynamically stable states. Comparatively, in dispersion of cubic Pd_2MnTi, the phonon modes of transverse acoustic (TA) at low frequency along G–X–W direction show noticeable softening tendency. However, the TA modes in tetragonal Pd_2MnTi are hard, suggesting more stable state. Comparative analysis suggests that the Pd_2MnTi could reach a dynamically stable state by martensitic phase transition, which agrees with the result from the calculated energy in Fig. 1(a). The partial phonon density of states (DOS) of Pd_2MnTi was also calculated and illustrated in Figs. 2(b) and 2(d). They could help further identify the origin of phonon modes softening. The primary factor separating the order of atomic contributions to phonon dispersions is weight. Typically, lower-frequency phonon modes are dominated by heavier atoms, and vice versa. In tetragonal Pd_2MnTi with $c/a = 1.4$, the normal sequence is displayed by the atomic contribution to phonon dispersions, leading to stable states devoid of observable softening. On the other hand, Ti atoms predominate in the medium frequency phonon dispersions in cubic Pd_2MnTi, locating beneath the optical modes of heavier Mn. The low-lying transverse acoustic phonon modes are deeply softened as a result of this inversion, which serves as a repulsive force on the acoustic modes through hybridization.[3,4]

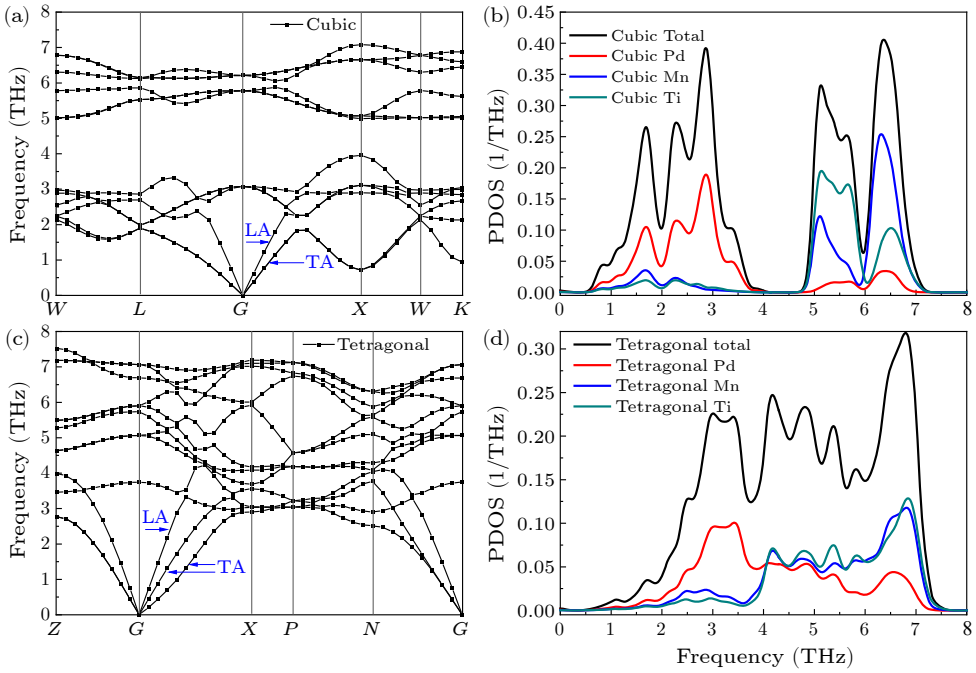

Fig. 2. (a) Calculated phonon dispersion of cubic Pd_2MnTi. The high-symmetry q point path in the Brillouin zone is selected as follows: $W(0.5, 0.25, 0.75) \rightarrow L(0.5, 0.5, 0.5) \rightarrow G(0, 0, 0) \rightarrow X(0.5, 0, 0.5) \rightarrow W(0.5, 0.25, 0.75) \rightarrow K(0.375, 0.375, 0.75)$. (c) Calculated phonon dispersion of tetragonal Pd_2MnTi. The absence of imaginary frequencies indicates the stability of the tetragonal phase. The high-symmetry q point path is selected as follows: $Z(0.5, 0.5, -0.5) \rightarrow G(0, 0, 0) \rightarrow X(0, 0, 0.5) \rightarrow P(0.25, 0.25, 0.25) \rightarrow N(0, 0.5, 0) \rightarrow G(0, 0, 0)$ in the Brillouin zone. [(b), (d)] The site projected phonon density of states (PDOS) of cubic and tetragonal Pd_2MnTi, respectively. They help identify the distribution of amplitudes of atoms in the frequency range. In cubic Pd_2MnTi, the visible anomalous behavior of medium frequencies phonon dispersions of Ti on $4a(0, 0, 0)$ sites, which lie below the optical modes of the heavier Mn on $4b(0.5, 0.5, 0.5)$ sites, is to act via hybridization as a repulsive force on the transverse acoustic modes.

By calculating the energy and phonon dispersions, the occurrence of martensitic phase transition could be prospective in Pd_2MnTi. In the following, electronic structure evolution during martensitic phase transition will be discussed in details.

Figure 3 illustrates the electronic DOS of Pd_2MnTi with $c/a = 0.85$, 1.0 and 1.4, respectively. The DOS could help ascertain the phase stability and to reveal the behind physical origin. First, in Fig. 3(a), one can find that the total DOSs of Pd_2MnTi with $c/a = 0.85$, 1.0 and 1.4 in spin-down direction distribute in the similar way near the Fermi level. However, their total DOSs in the spin-up direction show different characteristics. In cubic Pd_2MnTi, there is peak-like distribution near the Fermi level. This means an electronically unstable state.[32] By comparison of partial DOSs of Pd, Mn and Ti atoms, one can find that this peak-like distribution originates from the inter-atomic hybridization of Pd and Ti. However, this peak-like distribution is not sharp as the cases in conventional Heusler compounds, which results from the strong p–d covalent hybridization between p-electrons of main-group elements and d-electrons of transition metals.[32,33] When main-group elements were replaced by early transition metal atoms, such as the Ti atom in current Pd_2MnTi,

the original covalent hybridization was enormously weakened. Meanwhile the metallic bond character was enhanced due to the d–d hybridization between Pd and Ti atoms. Thus, the sharp DOSs distribution character near the Fermi level was degraded. The d–d metallic bond becomes dominant in Pd_2MnTi. The investigations in literature about Heusler compounds indicated that a tetragonal lattice distortion can help to remove the singularity of DOSs near the Fermi level.[32,34] In Fig. 3(a), the DOSs of tetragonal Pd_2MnTi with both $c/a = 0.85$ and $c/a = 1.4$ near the Fermi level become flattened. A pseudo energy gap appears near the Fermi level, indicating the generation of directional covalent bonds. Around the Fermi level, the DOS values also decrease noticeably. These characteristics support the stronger covalent bond in tetragonal Pd_2MnTi. The enhancement of inter-atomic chemical bonds can increase the inter-atomic hybridization level and stabilize the tetragonal phases. Comparatively, the much broader pseudo energy gap and smaller DOS values near the Fermi level suggest a more stable state in tetragonal Pd_2MnTi with $c/a = 1.4$. By martensitic phase transition, the tetragonal deformation of lattice promotes the re-distribution of electrons. The stronger chemical bond, such as covalent bond in this case, can be formed to strengthen inter-atomic bonding and consequently to enhance phase stability.

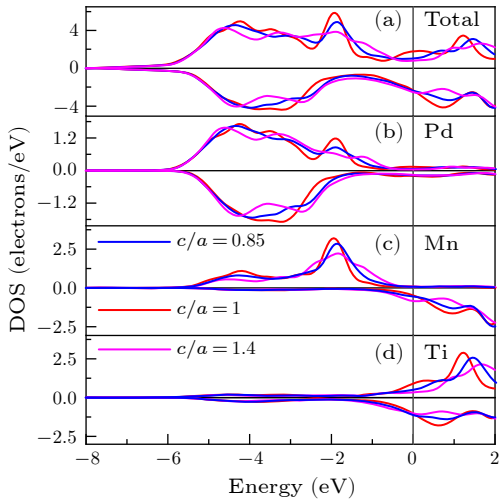

Fig. 3. Theoretical total spin-projected DOS plots of Pd_2MnTi with $c/a = 0.85$, 1.0 and 1.4 (a). The partial DOSs for d-electrons of atoms on specific crystalline site are shown in (b)–(d). The upper halves of each panel indicates the spin-up states.

Theoretical calculations of elastic constants and related parameters could judge phase stability, ductility, and also provide chemical bond information. Thus, it was widely used to discuss the phase stability and to reveal the related physical mechanism in Heusler compounds.[3,4,35,36] The calculated elastic constants and related parameters of cubic and tetragonal Pd_2MnTi are obtained as listed in Table 1. In cubic Heusler compounds, the following conditions guarantee its mechanical stability,[37] i.e., $C_{11} > 0$, $C_{44} > 0$, $C_{11} + 2C_{12} > 0$, and $C' = (C_{11} - C_{12})/2 > 0$. For cubic Pd_2MnTi, there are only three independent elastic constants. The calculated values of C_{11}, C_{12}, and C_{44} are 149.78, 145.09, and 73.41 GPa, respectively. Obviously, they can meet the first three conditions. For $C' = (C_{11} - C_{12})/2$, the value is only 2.345 GPa. When comparing the C' in well-known Heusler compounds,[3,4,35] this near zero C' suggests that phase transition may occur when external stimuli is applied on Pd_2MnTi. When it comes to tetragonal Pd_2MnTi with $c/a = 1.4$, one can find that it well satisfies the mechanical stability conditions for tetragonal structure:[38] $C_{11} > 0$, $C_{33} > 0$, $C_{44} > 0$, $C_{66} > 0$, $C_{11} - C_{12} > 0$, $C_{11} + C_{33} - 2C_{13} > 0$, and $2(C_{11} + C_{12}) + C_{33} + 4C_{13} > 0$. However, in tetragonal Pd_2MnTi with $c/a = 0.85$, the comparative analysis of obtained elastic constants in Table 1 indicates that it is less stable than that in high c/a tetragonal structure.

Table 1. Theoretical elastic constants C_{ij}, bulk modulus (B), shear modulus (G), Young's modulus (E), Poisson's ratio (υ), B/G ratio, Debye temperature and Vickers hardness (H_V) of Pd_2MnTi compounds.

c/a	Units	0.85	1.0	1.4
C_{11}	GPa	247.65	149.78	173.05
C_{33}	GPa	233.99		208.35
C_{44}	GPa	64.70	73.41	74.23
C_{66}	GPa	−8.13		79.75
C_{12}	GPa	68.60	145.09	111.32
C_{13}	GPa	104.30		96.68
B	GPa	142.63	146.66	129.31
G	GPa	54.40	44.98	62.29
E	GPa	144.78	122.43	161.02
ν		0.33	0.36	0.29
B/G		2.62	3.26	2.08
Debye temperature	K	340.03	310.81	362.17
H_V	GPa	5.21	3.55	7.47

Based on the calculated elastic constants, the Debye temperature is obtained as listed in Table 1. Generally, the higher Debye temperature means the stronger covalent bond, and vice versa. This method has been widely used in Heusler compounds, and published studies have verified its validness.[3,4,35,39] In Table 1, the Debye temperatures of cubic and tetragonal structures with $c/a = 0.85$ and $c/a = 1.4$ are 310.81, 340.03, and 362.17 K, respectively. Herein, the higher Debye temperatures in tetragonal structures indicate that the covalent bond in tetragonal phase is stronger. The stronger chemical bond just means the higher interatomic coupling and more stable states in tetragonal phases. Further comparative analysis of the Debye temperature of tetragonal phase indicates that the tetragonal Pd_2MnTi with $c/a = 1.40$ is much stronger in chemical bond and consequently a more stable state. The judgment on phase stability well agrees with that from the lattice size and lattice distortion dependent energy in Fig. 1(a). Additionally, the increased covalent hybridization would harden the elastic moduli. As a result, the highest shear modulus and Young's modulus were observed in high c/a tetragonal structure. The smallest values of shear modulus and Young's modulus are

shown in cubic Pd_2MnTi. The medium shear modulus and Young's modulus in tetragonal Pd_2MnTi with $c/a = 0.85$ indicate a medium chemical bond strength and metastable state.

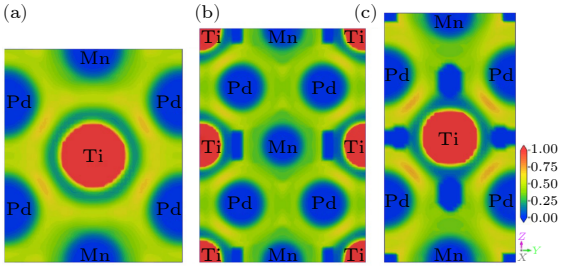

Fig. 4. Electron localization function distributions of Pd_2MnTi on (100) plane of unit cell of tetragonal structure with $c/a = 0.85$ (a) and $c/a = 1.40$ (c), and on (110) plane of unit cell of cubic structure (b). The scale bar from blue to red correlates to increased electron localization (i.e., greater covalent bonding). Comparatively, there is stronger covalent bonding in tetragonal Pd_2MnTi with $c/a = 1.40$.

Herein, the covalent bond characteristics in Pd_2MnTi are discussed by qualitative and quantitative ways. The electron localization function (ELF) distribution serves as a qualitative way to vividly reveal interatomic hybridization character in solids. Figure 4 show the ELF distribution of cubic and tetragonal Pd_2MnTi. Comparatively, the ductile properties of all-*d*-metal Heusler compounds are improved. This improvement results from the interatomic *d*–*d* hybridization, which is metallic. In current cubic Pd_2MnTi, the electron dispersion is relatively homogeneous. The *d*–*d* metallic bond is dominated. The covalent hybridization is weak, supported by the lower electrons accumulation level. Comparatively, there is the highest electrons accumulating level in tetragonal phase with $c/a = 1.4$. Details can be found in Fig. 4(c). It clearly supports a stronger covalent bond. Moreover, based on the quantum theory of atoms in molecules,[40,41] the charge-density topology is a quantitative method to quantify the charge distribution in Pd_2MnTi compounds with different c/a ratio. Following this method, the covalent character of Pd_2MnTi can also be determined by figuring out the charge on particular atoms in their sublattice. They are $(Pd^{0.21})_2(Mn^{-0.24}Ti^{0.18})$, $(Pd^{0.19})_2(Mn^{-0.21}Ti^{0.17})$ and $(Pd^{0.22})_2(Mn^{-0.25}Ti^{0.19})$ when $c/a = 0.85$, 1.0 and 1.40, respectively. Comparatively, Pd_2MnTi with $c/a = 1.4$ shows relatively higher covalent character. The weakest covalent character could occur in cubic Pd_2MnTi. The metallic bond would be enhanced as a compensation for the decreased covalent bond. The consistent conclusions are achieved based on qualitative and quantitative methods.

In solids, the crystal structures have important influences on the mechanical properties. The inherent factor to link crystal structure and mechanical properties is chemical bond. Physically, owing to the inherit nature of covalent bond, the compounds with stronger covalent component could possess the higher hardness. Herein, the Vickers hardness of Pd_2MnTi is calculated by $H_V = 0.92k^{1.137}G^{0.708}$, in which k is the G/B ratio.[42] The calculated H_V values are collected in Table 1. As is expected, the tetragonal martensitic phases show higher hardness than that of cubic phase. Especially, in Pd_2MnTi with $c/a = 1.4$, the highest hardness could reach 7.47 GPa. It supports the stronger covalent hybridization in tetragonal martensitic phases. Meanwhile, in cubic intermetallic compound Pd_2MnTi, the metallic bond would balance the decreased covalent bond. The stronger metallic bond in cubic phase enable the compound to possess better ductility. Thus, higher Poisson's ratio and B/G ratio are shown for cubic Pd_2MnTi. Empirically, the well adopted Poisson's ratio to distinguish between ductile and brittle materials is 0.33.[43] Physically, the covalent bond-dominated compounds are hard and brittle while the metallic bond-dominated materials are soft and ductile. Thus, this value can also work as a line to distinguish between covalent and metallic bonds. Fortunately, the Poisson's ratio in cubic Pd_2MnTi is 0.36, which is higher than the critical line. In the case of tetragonal Pd_2MnTi with $c/a = 1.4$, Poisson's ratio is 0.29, lower than the critical line. For the metastable tetragonal Pd_2MnTi with $c/a = 0.85$, Poisson's ratio is just 0.33, indicating a medium state. Thus, the mechanical parameters, such as hardness and ductility, support a stronger covalent hybridization in tetragonal martensitic phase.

From the above calculated chemical bond information, one can describe the nature of martensitic phase transition in Pd_2MnTi. It is a process, where the weaker metallic-type bonds in parent cubic phase are broken and stronger covalent-type bonds are formed. This would enhance interatomic hybridization strength and lower the energy of materials. By this transition, a more stable state could be achieved. Consequently, the possible martensitic phase transition would occur in Pd_2MnTi.

In this study, taking Pd_2MnTi as a representative example, the electronic structure evolution and correspondingly the nature of martensitic phase transition in all-*d*-metal Heusler compounds are systematically studied and revealed theoretically. The calculated lattice size and lattice distortion level-dependent energy suggest that the martensitic phase transition from high symmetric cubic phase to low symmetric tetragonal phase could occur in Pd_2MnTi, which is characterized by a large volume shrinkage and lattice distortion. The further comparative analysis of the calculated elastic constant related modulus and parameters, the electron localization function distribution, and electronic DOSs indicates that the volume shrinkage and lattice distortion promote the re-distribution of electrons, and result in a higher electron accumulation between the first nearest neighboring Pd and Ti atomic pairs in tetragonal phases. The enhanced covalent bond indicates the inter-atomic hybridization becomes stronger and correspondingly the tetragonal phase becomes more stable than the cubic phase. Based on the analysis of electronic structure evolution, thus the current study about Pd_2MnTi suggests that the nature of martensitic phase transition is a

process, in which the covalent-type strong chemical bond is established by breaking the original metallic-type bonds to stabilize the low symmetric phase. This study could help to deepen the understanding of the martensitic phase transition and the exploration of novel materials for potential technical applications.

Acknowledgements. This work was supported by the special fund for introduced talent to initiate scientific research in Nanjing Tech University, the National Natural Science Foundation of China (Grant Nos. 52088101 and 52325201), and the National Key Research and Development Program of China (Grant No. 2023YFA1607400). We are grateful to the High-Performance Computing Center of Nanjing Tech University for supporting the computational resources.

References

[1] Graf T, Felser C, and Parkin S S P 2011 *Prog. Solid State Chem.* **39** 1
[2] Wei Z Y, Liu E K, Chen J H, Li Y, Liu G D, Luo H Z, Xi X K, Zhang H W, Wang W H, and Wu G H 2015 *Appl. Phys. Lett.* **107** 022406
[3] Li G J, Xu L, and Cao Z H 2023 *Phys. Rev. Mater.* **7** 104411
[4] Li G J, Liu E K, Wang W H, and Wu G H 2023 *Phys. Rev. B* **107** 134440
[5] He P, Yang J, Ren Q, Wang B, Wu G, and Liu E 2024 *Chin. Phys. B* **33** 077201
[6] Peng L, Zhang Q, Wang N *et al.* 2023 *Chin. Phys. B* **32** 17102
[7] Lv T, Li G, Sun Q, and Zheng Y 2024 *J. Mater. Chem. C* **12** 13562
[8] Li G J, Liu E K, and Wu G H 2022 *J. Alloys Compd.* **923** 166369
[9] Li G, Xu L, and Cao Z 2024 *Phys. Chem. Chem. Phys.* **26** 8318
[10] Yan H L, Wang L D, Liu H X, Huang X M, Jia N, Li Z B, Yang B, Zhang Y D, Esling C, Zhao X, and Zuo L 2019 *Mater. Des.* **184** 108180
[11] Zhang G, Wang H, Li Z, Yang B, Yan H, Zhao X, and Zuo L 2023 *Scr. Mater.* **234** 115584
[12] Sun S, Bai J, Gu J, Guo K, Morley N, Gao Q, Zhang Y, Esling C, Zhao X, and Zuo L 2024 *J. Alloys Compd.* **976** 173406
[13] Guan Z Q, Bai J, Zhang Y, Gu J L, Morley N, Zhang Y D, Esling C, Zhao X, and Zuo L 2023 *Mater. Today Phys.* **36** 101183
[14] Cong D Y, Xiong W X, Planes A, Ren Y, Mañosa L, Cao P Y, Nie Z H, Sun X M, Yang Z, Hong X F, and Wang Y D 2019 *Phys. Rev. Lett.* **122** 255703
[15] Wei Z Y, Liu E K, Li Y, Han X L, Du Z W, Luo H Z, Liu G D, Xi X K, Zhang H W, Wang W H, and Wu G H 2016 *Appl. Phys. Lett.* **109** 071904
[16] Wei Z, Shen Y, Zhang Z, Guo J, Li B, Liu E, Zhang Z, and Liu J 2020 *APL Mater.* **8** 051101
[17] Liu J 2023 *Innov. Mater.* **1** 100031
[18] Romero-Muñiz C, Law J Y, Revuelta-Losada J, Moreno-Ramírez L M, and Franco V 2023 *Innov. Mater.* **1** 100045
[19] Zhang F Q, Batashev I, van Dijk N, and Brück E 2022 *Phys. Rev. Appl.* **17** 054032
[20] Zhang F, Wu Z, Wang J, Chen W, Wu Z, Chi X, Zhao C, Eijt S, Schut H, Bai X, Ren Y, van Dijk N, and Brück E 2024 *Acta Mater.* **265** 119595
[21] Wu M, Zhou F, Khenata R, Kuang M, and Wang X 2020 *Front. Chem.* **8** 546947
[22] Zhang S H, Wang Q, Kawazoe Y, and Jena P 2013 *J. Am. Chem. Soc.* **135** 18216
[23] Silvi B and Savin A 1994 *Nature* **371** 683
[24] Vanderbilt D 1990 *Phys. Rev. B* **41** 7892
[25] Perdew J P, Burke K, and Ernzerhof M 1996 *Phys. Rev. Lett.* **77** 3865
[26] Feng L, Guo C C, Zhang X Y, Xuan H C, Wang W H, Liu E K, and Wu G H 2018 *Chin. Phys. Lett.* **35** 038101
[27] Xu L, Li G, and Cao Z 2024 *J. Magn. Magn Mater.* **590** 171637
[28] Liu Y, Lyu M, Liu J, Zhang S, Yang J, Du Z, Wang B, Wei H, and Liu E 2023 *Chin. Phys. Lett.* **40** 047102
[29] Lyu M, Liu Y, Zhang S, Liu J, Yang J, Wang Y, Feng Y, Dong X, Wang B, Wei H, and Liu E 2024 *Chin. Phys. B* **33** 107507
[30] Bao L F, Huang W D, and Ren Y J 2016 *Chin. Phys. Lett.* **33** 077502
[31] Zeng Q, Shen J, Liu E, Xi X, Wang W, Wu G, and Zhang X 2020 *Chin. Phys. Lett.* **37** 076101
[32] Faleev S V, Ferrante Y, Jeong J, Samant M G, Jones B, and Parkin S S P 2017 *Phys. Rev. Appl.* **7** 034022
[33] Opeil C P, Mihaila B, Schulze R K, Mañosa L, Planes A, Hults W L, Fisher R A, Riseborough P S, Littlewood P B, Smith J L, and Lashley J C 2008 *Phys. Rev. Lett.* **100** 165703
[34] Winterlik J, Chadov S, Gupta A, Alijani V, Gasi T, Filsinger K, Balke B, Fecher G H, Jenkins C A, Casper F, Kübler J, Liu G D, Gao L, Parkin S S P, and Felser C 2012 *Adv. Mater.* **24** 6283
[35] Li G J, Xu L, and Cao Z H 2023 *J. Mater. Chem. C* **11** 6173
[36] Li G, Liu E, Liu G, Wang W, and Wu G 2021 *Chin. Phys. B* **30** 83103
[37] Mouhat F and Coudert F X 2014 *Phys. Rev. B* **90** 224104
[38] Nye J F 1985 *Physical Properties of Crystals* (Oxford: Oxford University Press)
[39] Li G J, Liu E K, Wang W H, and Wu G H 2023 *J. Alloys Compd.* **956** 170389
[40] Henkelman G, Arnaldsson A, and Jónsson H 2006 *Comput. Mater. Sci.* **36** 354
[41] Bader R F W 1990 *Atoms in Molecules-A Quantum Theory* (Oxford: Oxford University Press)
[42] Tian Y, Xu B, and Zhao Z 2012 *Int. J. Refract Met. Hard Mater.* **33** 93
[43] Frantsevich I N, Voronov F F, and Bokuta S A 1983 *Elastic Constants and Elastic Moduli of Metals and Insulators Handbook* (Kiev: Naukova Dumka)